RESEARCH ON MULTI-STAGE HEATING METHOD OF HIGH SPEED RAILWAY EMERGENCY TRACTION BATTERY SYSTEM BASED ON FLAT HEAT PIPE

by

Xudong SUN [a], ***Xiaoming XU*** [a*], ***Wei TANG*** [a], ***Huifen JIN*** [b], ***and Hua DING*** [a]

[a] School of Automotive and Traffic Engineering, Jiangsu University, Zhenjiang, China
[b] Tianjin Lishen Battery Joint-Stock Co., Ltd., Tianjin, China

Original scientific paper
https://doi.org/10.2298/TSCI200118172S

High speed rail vehicles need to start the emergency traction battery system in an emergency. In order to ensure that the emergency traction battery system can be quickly started in cold conditions and ensure that the high speed railway has sufficient mileage, this paper proposes a multi-stage heating method based on flat heat pipes. The thermodynamic parameters of the power battery are obtained by simulation analysis and experimental verification. According to the thermodynamic model, the heat generation model and coupled heat transfer model of the battery are established. Different heating powers are assigned to different heating points and the total heating power is kept constant. Through the analysis results, the multi-stage heating device of the emergency traction battery system can effectively reduce the heating time under cold conditions and the temperature difference between the battery system Modules. This paper can provide reference to the design of the battery pack and the matching of the heating system.

Key words: *high speed railway, emergency traction battery system, flat heat pipe, lithium-ion battery, multi-stage heating*

Introduction

High speed railways use electric energy as their energy source. It is inevitable that high speed railways cause short-term interruptions or prolonged breakdowns of power supply in the construction and operation stage due to many reasons [1]. The emergency traction battery system can be towed and driven by the battery itself and ensures that high speed rail vehicles can travel to the nearest station [2].

At present, lithium-ion batteries have become the most widely used secondary batteries because of their high energy density and long cycle life. Lithium-ion power batteries have become mainstream in the market [3, 4]. For ensuring short enough residence time and long enough cruising range under emergency conditions for high speed railways emergency traction system, lithium-ion battery should be selected as the power source of high speed railway emergency traction battery system. When lithium-ion batteries are used as the power batteries for an electric vehicle, local overheating may occur during operation. Before de-

* Corresponding author, e-mail: 1683893602@qq.com

signing a good battery thermal management system, the heating characteristics and temperature control of the batteries should be considered [5, 6]. Whether it is low temperature or high temperature will gradually reduce the cycle life of lithium-ion batteries, the most suitable operating temperature range for lithium-ion batteries is 15~40 °C. Effective battery thermal management is important to maintain battery performance and prevent thermal runaway [7]. Xu *et al.* [5] have conducted extensive research on the air cooling of the battery pack. As a result, it was found that the maximum temperature rise and the internal maximum temperature difference of the battery pack with vent holes were reduced by about 23.1% and 19.9% . In addition, the double *U*-type air duct has better heat dissipation effect on the battery pack than the double 1-type duct [8]. Flat heat pipe is also applied to battery thermal management system. Qu *et al.* [9, 10] designed a hybrid flexible oscillating heat pipe (FOHP), the result showed that FOHP works well and has high space flexibility and acceptable heat transfer performance.

However, the low temperature discharge characteristics of lithium-ion batteries were not ideal. With the decrease of temperature, the discharge voltage and discharge capacity of the battery were significantly reduced especially below 253 K (–20 °C). When the temperature was as low as 233 K (–40 °C), the battery could not discharge at a constant current of 30 A. In order to ensure that the battery pack of the emergency traction battery system can be normally discharged under extremely low temperature environment, the battery pack needed to be heated. Low temperature heating of lithium-ion batteries had been studied by some scholars [11-14]. Shuai *et al.* [15] proposed the self-limiting temperature heating method that was a strip-like constant temperature electric heating material. When the heating temperature reached 75 °C, the heating cable was in a high impedance state, the current was infinitesimal and the auxiliary heat was automatically suspended. Lei *et al.* [16] proposed a wide-wire metal film heating method in which a copper film was coated on both sides of a wide-line metal film and the battery was heated through a copper film to generate resistance heat through a current to heat the battery at a low temperature. Luo *et al.* [17] proposed a heating system consisting of a heating source electric heating film, a heat transfer medium transformer oil and a thermal insulation layer silica aerogel plate. Stuart and Hande [18] designed a heating method that heated the lithium battery and used a 60 Hz low frequency alternating current to heat the nickel-metal hydride battery against a lead-acid battery and 10~20 kHz high frequency current. Salameh and Alaoui [19] used the Peltier effect to conduct heating experiments on the batteries of electric vehicles. Li *et al.* [20] placed the thermistor heating tape on the inner wall of the battery pack and heated the lithium battery pack through heat transfer. This method had many advantages such as no overheating, safety, reliability, energy conservation, and rapid temperature rise. Pan and Guo [21] applied an electric heating film to a single side of each battery cell for heating and the heating effect was better, but the heat dissipation of the monomer was affected. Zhang *et al.* [22] attached a wide-line metal film to the two larger sides of the battery cell for heating. The temperature uniformity and heating efficiency of the method were better, but it was necessary to accurately control the system, which will affect to a certain extent heat dissipation of the battery cells. These low temperature heating schemes of lithium-ion batteries had the following problems. Firstly, the lithium-ion battery may not be discharged at a very low temperature and these low temperature heating schemes may cause heating of the lithium-ion battery out of balance and reduce the discharge capacity of lithium-ion batteries. Therefore, the emphasis of this paper was designing a heating method to ensure that the emergency traction battery system can work as quickly as possible at extremely low ambient temperature.

Experimental determination of battery

The thermodynamic parameters

As a heat source for battery packs, the heat generating power per unit volume of a lithium-ion battery is referred to as heat generating rate. The heat generation power of the battery cell can be calculated according to the general model of battery heating established by Bernardi *et al.* [23]:

$$\Phi = \left(\sum_i I_i E_{i,\mathrm{avg}} - IE \right) - \sum_i I_i T \frac{\mathrm{d}E_{i,\mathrm{avg}}}{\mathrm{d}T} \tag{1}$$

where Φ is the heat generating power of the battery cell, I – the charge and discharge current, I_i – the i^{th} layer electrode corresponding charging and discharging current, E – the battery cell load voltage, $E_{i,\,avg}$ – the open-circuit voltage of the i^{th} layer electrode, and T – the battery temperature.

Since I and I_i are equal in size, the aforementioned equation can be further simplified:

$$\Phi = I\left[\left(E_0 - E \right) - T \frac{\mathrm{d}E_0}{\mathrm{d}T} \right] \tag{2}$$

where E_0 is the cell open circuit voltage and E – the cell load voltage.

In addition, $(E_0 - E)$ can be expressed by the product of ohmic resistance and current:

$$E_0 - E = IR_\mathrm{s} \tag{3}$$

$$\Phi = I^2 R_\mathrm{s} - IT \frac{\mathrm{d}E_0}{\mathrm{d}T} \tag{4}$$

where $\mathrm{d}E_0/\mathrm{d}T$ is the coefficient of variation of battery voltage with temperature, considering it as a constant for a certain type of battery.

A 55 Ah lithium-ion battery is selected, whose characteristic parameters are shown in tab. 1.

Table 1. Characteristic parameters of this lithium-ion battery cell

Ingredient	Density [kgm^{-3}]	Specific heat capacity [Jkg^{-1}K^{-1}]	Thermal conductivity [Wm^{-1}K^{-1}]
Cell	2124.5	912.8	30.4
Anode	8979.1	381.4	387.3
Cathode	2718.6	870.8	203.1
Case	8193.9	439.0	14.6
Separator	1008.3	1977.8	0.335

Battery cell experimental determination

In order to measure the surface temperature of the battery during charging and discharging, five temperature measuring points were arranged, three of which were placed on the side walls and two were placed at the bottom. In order to prevent the ambient temperature from causing interference to the test data measurement, the battery cells are placed in an incubator, and the incubator is composed of three layers of heat insulating material [24].

The calorific value is calculated:

$$Q = c_p m \nabla T \tag{5}$$

where Q is the calorific value, c_p – the specific heat capacity, m – the object mass, and ∇T – the temperature change value.

The heating power of the battery can be obtained:

$$P = \frac{c_p m \nabla T}{t} \tag{6}$$

where P is the heating power and t – the time.

Test process: adjust the incubator to the appropriate temperature, charge to 3.65 V at a certain rate, turn to constant voltage charge, to 0.05 [C] cut off; then discharge to 2.50 V cut off at this rate.

Figure 1 shows the curve of temperature as a function of time of the cell when charged and discharged at the rate of 0.5 [C].

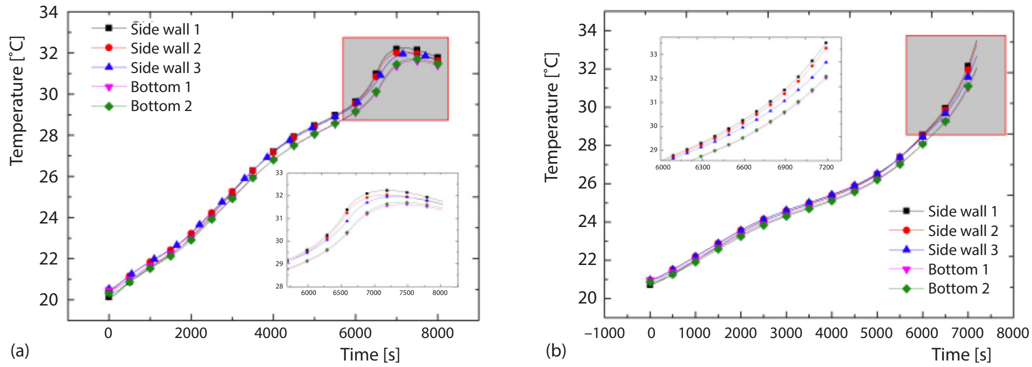

Figure 1. The curve of temperature as a function of time of the cell when charged and discharged at 0.5 [C]; (a) charging process and (b) discharging process

The temperature data and heating power of the battery charged and discharged at different rates are shown in tab. 2. As can be seen from tab. 2, the heating power of the battery cells increases as the charge and discharge rate increases.

Table 2. The temperature data and heating power of the battery charged and discharged at different rates

Working condition	Charge			Discharge		
Rate [C]	Original temperature [°C]	End temperature [°C]	Heating power [W]	Original temperature [°C]	End temperature [°C]	Heating power [W]
0.5	20.39	31.40	2.06	20.19	32.01	2.55
1.0	19.92	35.43	5.42	20.05	37.39	7.60
1.5	20.22	43.16	10.06	20.37	44.49	15.60
2.0	20.27	45.39	14.44	20.29	47.99	23.89

Model verification

When performing thermal analysis on the battery, the accuracy of the battery heat generation rate must be verified. Here, the battery simulation and experimental test results of the single cell at 20 °C ambient temperature, 1 [C] charge and discharge rate are compared. The thermal power of battery cell on charging and discharging process is the reference for the heat source setting on simulation calculation. Figure 2 shows the temperature field distribution of battery cell by simulation calculation, it could be seen that the temperature field distribution of battery cell on charging process is close to the discharging process, but the temperature of battery cell on discharging process is relatively higher, which could be seen from the temperature field distribution near the poles. As could be seen from fig. 3, the results calculated by simulation fit experiment test: the simulation value is 1.25 °C higher than experiment on charging process, and 1.00 °C higher than experiment on discharging process.

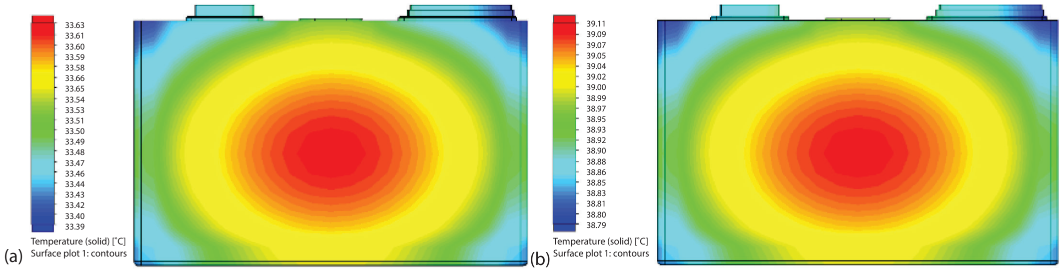

Figure 2. The temperature field distribution of lithium-ion battery cell on charging and discharging process; (a) charging process and (b) discharging process

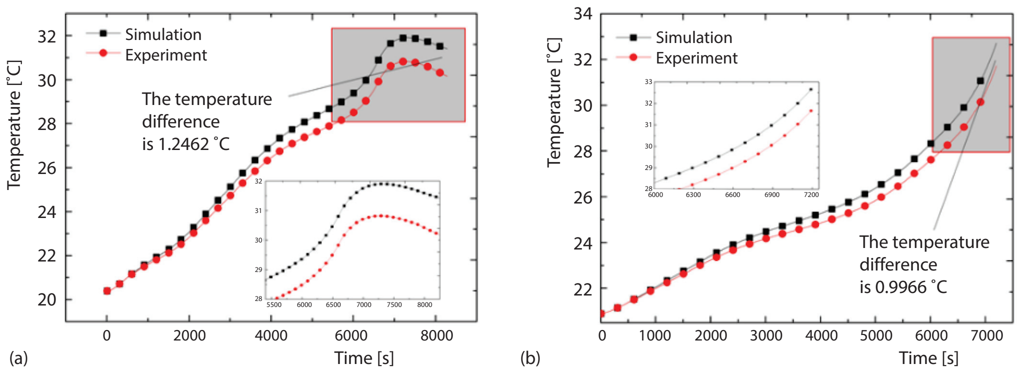

Figure 3. Comparison of temperature data by experiment and simulation; (a) charging process and (b) discharging process

Numerical computation methodology

Mathematical model

Battery heat generation model

Newman *et al.* [25] first proposed the general expression of the heating rate of lithium-ion batteries from the conservation of battery energy. In their model, heat generation is considered uneven, so an overall heat model was proposed:

$$Q = Q_i + Q_r = I(E - U) - IT\frac{\mathrm{d}E}{\mathrm{d}T} \tag{7}$$

where Q [W] is the overall heat generation rate of battery, Q_i – the heat generation rate of irreversible reaction, Q_r [W] – the heat generation rate of reversible reaction, U [V] – the open circuit voltage, I [A] – the current, E [V] – the balanced electromotive force, T [K] – the temperature of the battery.

It can be obtained from the classical heat conduction equation:

$$\rho C_\rho \frac{\partial T}{\partial t}=\frac{\partial}{\partial x}\left(k_x \frac{\partial T}{\partial x}\right)+\frac{\partial}{\partial y}\left(k_y \frac{\partial T}{\partial y}\right)+\frac{\partial}{\partial z}\left(k_z \frac{\partial T}{\partial z}\right)+q-q_{\mathrm{con}} \tag{8}$$

where ρ is the density, C_p – the specific heat capacity, T – the temperature, k_x, k_y are the lateral and longitudinal thermal conductivity of the electrode, respectively, q – the heat generation rate, and q_{con} – the heat dissipation rate.

In order to obtain a more accurate heat generation model for lithium ion batteries, improvements are made on the basis of the aforementioned heat generation model, considering the heat generation rate by adding a side reaction:

$$Q=Q_R+Q_p+Q_S+Q_j \tag{9}$$

where Q_R [W] is the reaction heat, Q_p [W] – the polarization heat, Q_s [W] – the side reaction heat, and Q_j [W] – the joule heat.

Heat conduction model of heat pipe

The evaporation section of flat heat pipe with microgrooves is heated and liquid evaporates into saturated steam at the vapor-liquid interface. Steam flows from the evaporation section along the axial direction of flat heat pipe to the condensation section under a slight differential pressure. The steam in the steam chamber condenses at the vapor-liquid interface of the liquid meniscus in the condensation section. After condensation, under the action of the capillary force, the condensed fluid-flows from the condensation section the evaporation section in the axial direction. The heat transfer rate can be calculated:

$$\dot{Q}=\dot{M}_C c_p (T_{c2}-T_{c1}) \tag{10}$$

where $\dot{M}c$ is the mass-flow rate of the cooling water, c_p – the special heat, T_{c1} and T_{c2} are the inlet and outlet temperature from condenser section.

The thermal resistance of heat pipe can be determined by the equation:

$$R=\frac{\dfrac{T_{E1}+T_{\mathrm{E2}}}{2}-\dfrac{T_{\mathrm{C1}}+T_{\mathrm{C2}}}{2}}{\dot{Q}_{\max}} \tag{11}$$

where T_{E1} and T_{E2} mean inlet and outlet temperatures from evaporator section and $\dot{Q}_{\max}$ – the maximum heat transfer rate.

Computational fluid mechanics governing equation

Mathematical expressions describing the mechanism of fluid dynamics are usually derived from the most basic physical principles. The most basic governing equations for fluid dynamics are the continuity equation, the momentum equation, and the energy equation.

The continuity equation follows the law of conservation of mass:

$$\frac{D\rho}{Dt}+\rho\left(\frac{\partial u}{\partial x}+\frac{\partial v}{\partial y}+\frac{\partial w}{\partial z}\right)=0 \tag{12}$$

where ρ [kgm^{-3}] is the fluid density, t [s] – the time, x, y, and z are the three dimensions of the Cartesian co-ordinate system, respectively, u, v, and w [ms^{-1}] – the fluid velocity in the direction of x, y, and z, respectively.

The momentum equation follows Newton's second law:

$$\begin{aligned}
&\rho\left(\frac{\partial u}{\partial t}+u\frac{\partial u}{\partial x}+v\frac{\partial u}{\partial y}+w\frac{\partial u}{\partial z}\right)=-\frac{\partial p}{\partial x}+\frac{\partial \tau_{xx}}{\partial x}+\frac{\partial \tau_{yx}}{\partial y}+\frac{\partial \tau_{zx}}{\partial z}+\rho f_x\\
&\rho\left(\frac{\partial v}{\partial t}+u\frac{\partial v}{\partial x}+v\frac{\partial v}{\partial y}+w\frac{\partial v}{\partial z}\right)=-\frac{\partial p}{\partial y}+\frac{\partial \tau_{yy}}{\partial y}+\frac{\partial \tau_{xy}}{\partial x}+\frac{\partial \tau_{zy}}{\partial z}+\rho f_y\\
&\rho\left(\frac{\partial w}{\partial t}+u\frac{\partial w}{\partial x}+v\frac{\partial w}{\partial y}+w\frac{\partial w}{\partial z}\right)=-\frac{\partial p}{\partial z}+\frac{\partial \tau_{zz}}{\partial z}+\frac{\partial \tau_{yz}}{\partial y}+\frac{\partial \tau_{xz}}{\partial x}+\rho f_z
\end{aligned} \tag{13}$$

where p [Pa] is the fluid pressure, τ_{xy} [Pa] – the stress acting on the x plane pointing to the y-direction, and f_x, f_y, f_z [ms^{-2}] are the acceleration in the direction of x, y, and z.

Physical model

This paper studied lithium-ion power batteries that were suitable for high speed railways emergency conditions. Figure 4 showed the position and structure of the study object on the high speed railway. The emergency traction battery system used 38.4 V/24 Ah standard high power battery Modules and 28 battery Modules were connected in series to form a 1075.2 V/24 Ah lithium-ion battery pack system. The object of this study was a square battery pack with a total of three Modules, as shown in fig. 4. With considering that the battery pole had little effect on the temperature, the battery model was simplified. In general, the gap between the batteries was small. Three battery Modules were placed on three flat heat pipes. Three heat pipes were installed below the Module and connected to the water pipes. In addition, the portion of the heating plate where the flat plate heat pipe was placed extended to the heating liquid pipe and the portion of the plate heat pipe that came into contact with the flat heat pipe performs thermal management of the battery through the coupling of the heating liquid and the heating chip.

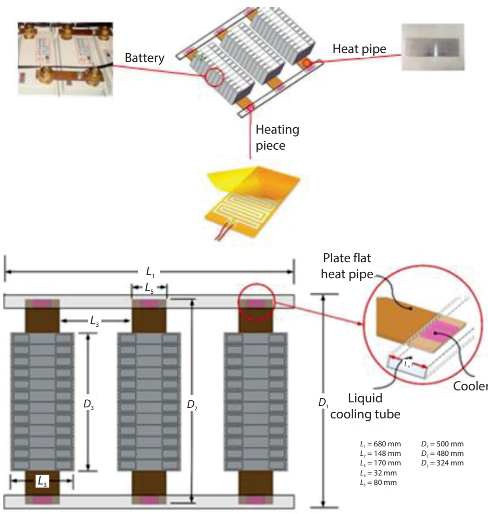

Figure 4. Overlook view of thermal management system model

Heating performance indexes

This paper selected the heating time and the temperature difference between the Modules as the evaluation index. Excessive heating time will increase the emergency traction start time of the high speed railways. In order to ensure the safety of high speed railways in emergency situations, the heating time of the Modules and the temperature difference between the Modules should be reduced as much as possible.

Result and discussion

Discharge rate of emergency traction battery system and discharge capacity were related to the temperature of the battery system. In the cold environment, the battery system heating needed to go through two processes: preheating and low temperature discharge heating.

This paper designed the following four heating modes: no heating point, a heating point, three heating points (the same heating power), three heating points (inconsistent power).

Heating performance indexes preheating process

Heating time required under various conditions during preheating is shown in tab. 3.

Table 3. Heating time required under various conditions during preheating [s]

	No heating point	One heating point	Three heating points (40 W, 40 W, 40 W)	Three heating points (30 W, 40 W, 50 W)
Module 1	684	684	641	650
Module 2	722	598	672	672
Module 3	758	746	703	692

The four heating modes studied in this paper are shown in fig. 5

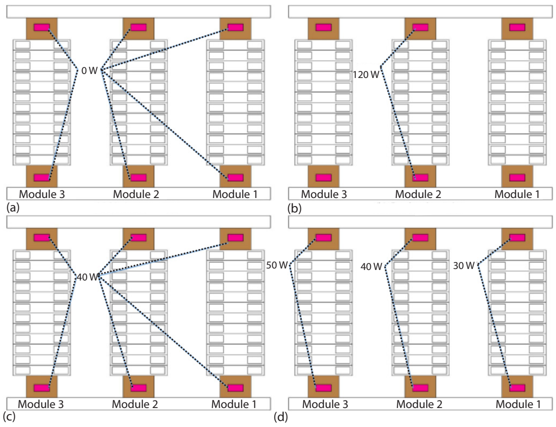

Figure 5. Four heating modes; (a) no heating point, (b) one heating point, (c) three heating points (40 W, 40 W, 40 W, 40 W), and (d) three heating points (30 W, 40 W, 50 W)

Temperature distribution between different Modules in the same heating mode

No heating point

According to tab. 3 and fig. 6(a), the heating time of the Module 2 was greater than the heating time of the Module 1 by 38 seconds, and the heating time of the Module 3 was greater than the heating time of the Module 2 by 36 seconds. The temperature difference between Module 2 and Module 1 was 1.23 °C, Module 3 and Module 2 was 1.17 °C, Module 3 and Module 1 was 2.39 °C at 680 seconds. These data indicate the following rules: Module 1 was first to 20 °C; the heating time difference and the temperature difference showed a kind of multiplier relationship. The reasons behind this phenomenon are as follows: Since the Module 1 was closest to the water inlet, the heat exchange between the heat pipe of the Module 1 and the heating liquid was most effective and the Module 1 first reached 20 °C; after heated fluid-flows through the Module 1, the temperature fell. The distance between the three Modules was equal, the temperature of the heating liquid dropped to the same extent and the temperature difference between the heating liquid and the Module was always large at this stage, so the heating time difference was roughly multiplied.

One heating point (arranged in the middle) 120 W

According to tab. 3 and fig. 6(b), the heating time of the Module 2 was greater than the heating time of the Module 1 by 86 seconds, and the heating time of the Module 3 was greater than the heating time of the Module 2 by 148 seconds. The temperature difference between Module 2 and Module 1 was 3.57 °C, Module 3 and Module 2 was 5.70 °C. Module 2 heating time was shortened by 124 seconds. These data indicate the following rules: Module 2 achieved –20 °C temperature requirements firstly; Module 3 heating time has not been significantly reduced; and the temperature difference between Modules has increased by 2.9 times and 4.9 times. The reasons behind this phenomenon are as follows: Although the temperature of heating fluid through the Module 2 below the temperature at which the flow through the Module 1, the temperature of the Module 2 rase rapidly to –20 °C under the 120 W heating piece. The thermal conductivity of the planar heat pipe was much larger than the thermal conductivity of the water, so the heating liquid did not take away part of the heat generated by the heating sheet to reduce the heating time of the Module 3.

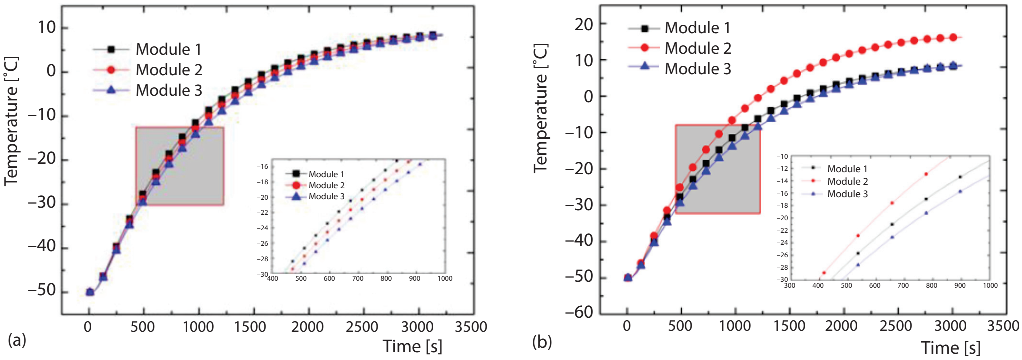

Figure 6. Heating curve under different heating conditions; (a) no heating point and (b) one heating point

Three heating points (40 W, 40 W, 40 W)

According to tab. 3 and fig. 7(a), the heating time of the Module 2 was greater than the heating time of the Module 1 by 31 seconds, and the heating time of the Module 3 was greater than the heating time of the Module 2 by 31 seconds. The temperature difference between Module 2 and Module 1 was 1.11 °C, Module 3 and Module 2 was 1.05 °C. When the heating time of Module heated to a temperature –20 °C reduced by 50 seconds approximately. When the Module 1 heat to –20 °C, the temperature difference between the three Modules reduced 8% and the heating time of three Modules had no great changes. The reasons behind this phenomenon are as follows: All the three Modules were placed on by a 40 W heating plate, which only reduced the heating time of the three Modules at the same time, but did not effectively reduce the time difference between the three Modules; the thermal conductivity of the planar heat pipe was much larger than the thermal conductivity of the water, so the temperature difference between the Modules did not change a lot; and since the heating power of the heating sheet was the same, the Module 1 was still the first to reach –20 °C.

Three heating points (30 W, 40 W, 50 W)

According to tab. 3 and fig. 7(b), the heating time of the Module 2 was greater than the heating time of the Module 1 by 22 seconds, and the heating time of the Module 3 was greater than the heating time of the Module 2 by 20 seconds. The temperature difference between Module 2 and Module 1 was: 0.74 °C, Module 3 and Module 2 was 0.67 °C. These data indicate the following rules: The heating time of Modules decreased by 45%; the Module 1 heated to 20°C firstly; and the temperature difference between the three Modules decreased by 34.4%. The reasons behind this phenomenon are as follows: As the heating liquid-flowed through the various Modules, the temperature of the heating liquid dropped, so that the heat transferred to the next Module was reduced. The heat received by the three Modules was at the same level by increasing the power of the heating point.

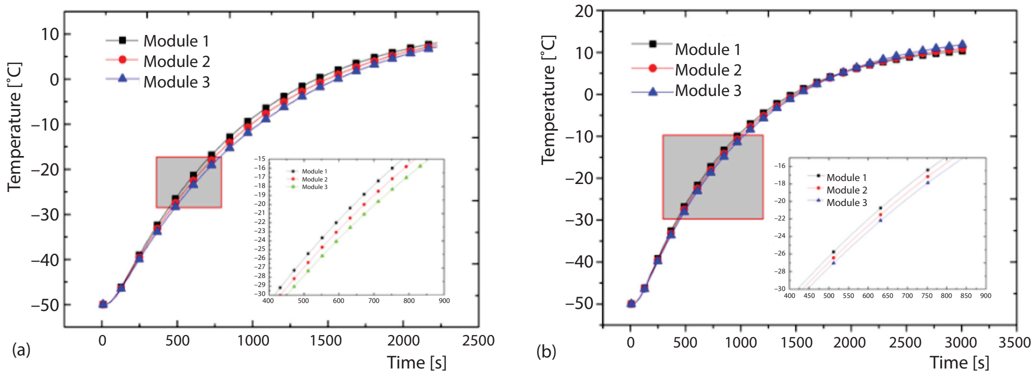

Figure 7. Heating curve under three heating points with different heating power; (a) 40 W, 40 W, 40 W and (b) 30 W, 40 W, 50 W

Low temperature discharge process

Heating time under various conditions during low temperature discharge is shown in tab. 4.

Table 4. Heating time required under various conditions during low temperature discharge [s]

	No heating point	One heating point	Three heating points (40 W, 40 W, 40 W)	Three heating points (30 W, 40 W, 50 W)
Module 1	1336	1336	1116	1164
Module 2	1404	890	1156	1158
Module 3	1478	1410	1194	1148

Temperature distribution between different Modules in the same heating mode

No heating point

According to tab. 4 and fig. 8(a), the heating time difference between Module 2 and Module 1 was 68 seconds and the heating time difference between Module 2 and Module 3 was 74 seconds. The temperature difference between Module 2 and Module 1 was 0.60 °C; the temperature difference between Module 3 and Module 2 was 0.60 °C; the temperature difference between Module 3 and Module 1 was 1.20 °C. The heating time of Modules under low temperature discharge was over 1000 seconds. Heating time difference between Modules exceeded 100 seconds. The temperature difference between Modules was small. The reasons behind this phenomenon are as follows. The temperature difference between the heating liquid and the Module was reduced, resulting in a decrease in heat transfer capability. The Module closed to the liquid inlet would absorb part of the heat of the heating liquid, causing the temperature of the heating liquid to decrease when it came into contact with the next Module of the heating liquid. In a sufficiently long period of time, the heat exchange was relatively sufficient and the temperature difference between the heating liquid and the Module was lowered, and the heat exchange capacity was weakened to further reduce the temperature difference between the Modules.

One heating point (arranged in the middle) 120 W

According to tab. 4 and fig. 8(b), the heating time difference between Module 2 and Module 1 was 446 seconds and the heating time difference between Module 2 and Module 3 was 520 seconds. The temperature difference between Module 2 and Module 1 was 6.62 °C; the temperature difference between Module 3 and Module 2 was 7.31 °C; the temperature difference between Module 3 and Module 1 was 0.69 °C. The heating time of Module 2 was 890 seconds which was less than 1404 seconds compared to the case without a heating point. The heating time of Module 3 was little changed. The temperature difference and the heating time difference between Module 2 and Module 1/Module 2, and Module 3 increased 1097% and 656% compared to the case without a heating point. The reasons is that the heat conduction efficiency of the planar heat pipe was far greater than the heat conduction efficiency of the water, and the heating liquid cannot take away the heat generated by the heating sheet.

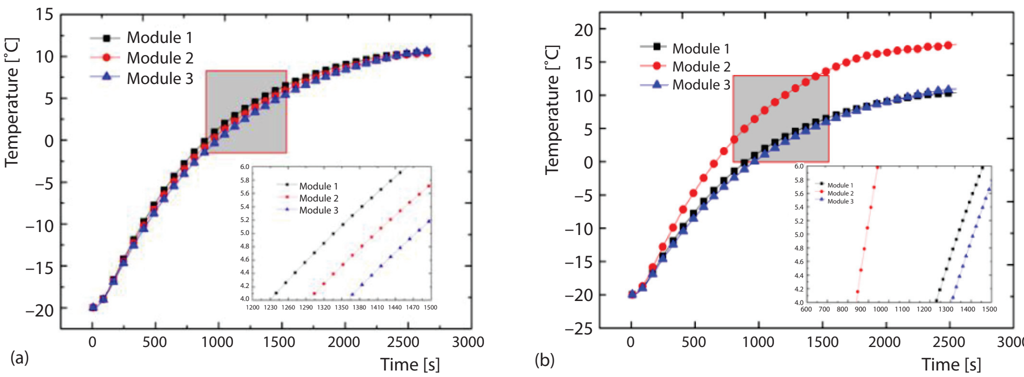

Figure 8. Heating curve under different heating conditions; (a) no heating point and (b) one heating point

Three heating points (40 W, 40 W, 40 W)

From tab. 4 and fig. 9(a), the heating time difference between Module 2 and Module 1 was 40 seconds and the heating time difference between Module 2 and Module 3 was 38 seconds. The temperature difference between Module 2 and Module 1 was 0.44 °C; the temperature difference between Module 3 and Module 2 was 0.50 °C; the temperature difference between Module 3 and Module 1 was 0.69 °C. The heating time of the three Modules was greatly shortened and the degree of reduction were 220, 248, and 284 seconds compared to the case without a heating point. The heating time difference and the temperature difference between the

Modules was greatly reduced compared to the case with a heating point. The reasons behind this phenomenon are as follows. The heat conduction efficiency of the planar heat pipe was far greater than the heat conduction efficiency of the water, so the effect of heating piece was more than the effect of heating liquid.

Three heating points (30 W, 40 W, 50 W)

According to tab. 4 and fig. 9(b), the heating time difference between Module 2 and Module 1 was 6 seconds and the heating time difference between Module 2 and Module 3 was 10 seconds. The temperature difference between Module 2 and Module 1 was 0.09 °C; the temperature difference between Module 3 and Module 2 was 0.10 °C; the temperature difference between Module 3 and Module 1 was 0.19 °C. Three Modules almost simultaneously reached the specified target temperature. The temperature difference between the three Modules was almost negligible. The reasons behind this phenomenon are as follows. As the heating liquid-flows through the various Modules, the temperature of the heating liquid dropped, so that the heat transferred to the next Module was reduced. The heat received by the three Modules was at the same level by increasing the power of the heating point.

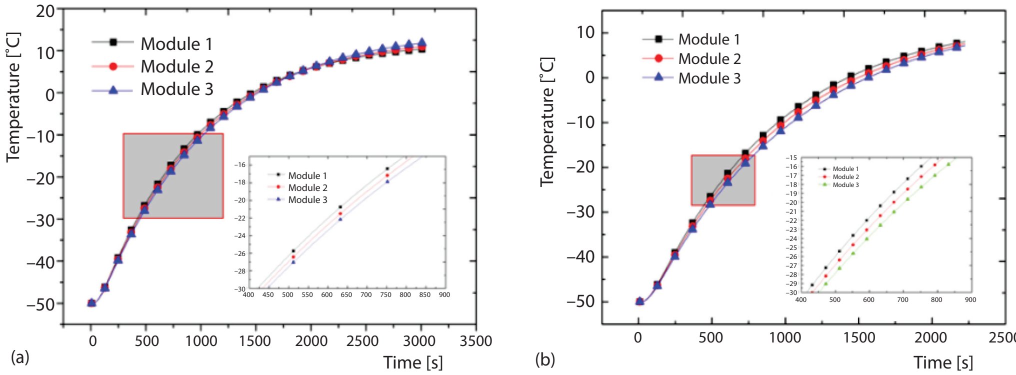

Figure 9. Heating curve under three heating points with different heating power; (a) 40 W, 40 W, 40 W and (b) 30 W, 40 W, 50 W

Conclusion

The multi-stage heating device of the emergency traction battery system the paper proposed can effectively reduce the heating time of the battery system in the high cold area and the temperature difference between the battery system Modules to ensure the emergency starting capacity and driving range of high speed railways. It was hoped that the conclusions can provide reference for the design and research of the heating process of emergency traction battery systems for high speed railways.

Acknowledgment

This work was supported by National Natural Science Foundation of China (51875259), National key research and development program (2018YFC0810504), Foundation of State Key Laboratory of Automotive Simulation and Control (20180103), Postgraduate Research & Practice Innovation Program of Jiangsu Province (SJCX19_1169).

References

[1] Jin, B., Intelligent Emergency Power Supply System Mounted on Rail Transit Vehicle, *Research on Urban Rail Transit*, *17* (2014), 12, pp. 118-123+130
[2] Shen, T., Zhou, Q., Implementation of Rail Transit Vehicle Emergency Battery Traction, *Research on Urban Rail Transit*, *19* (2016), 7, pp. 110-115
[3] Omar, N., *et al*., Lithium Iron Phosphate Based Battery – Assessment of the Aging Parameters and Development of Cycle Life Model, *Appl. Energy*, *113* (2014), Jan., pp. 1575-1585
[4] Sato, N., Thermal Behavior Analysis of Lithium-Ion Batteries for Electric and Hybrid Vehicles, *Journal of Power Sources*, *99* (2010), 1, pp. 70-77
[5] Xu, X., *et al*., Research on Heat Dissipation Performance and Flow Characteristics of Air-Cooled Battery Pack, *International Journal of Energy Research*, *42* (2018), 11, pp. 3658-3671
[6] Xu, X., *et al*., Research on the Heat Dissipation Performance of Lithium-Ion Cell with Different Operating Conditions, *International Journal of Energy Research*, *41* (2017), 11
[7] Pesaran, A. A., Battery Thermal Management in EV and HEV: Issues and Solutions, *Proceedings*, Advanced Automotive Battery Conference, Las Vegas, Nev., USA, 2001
[8] Xu, X., *et al*., The Forced Air Cooling Heat Dissipation Performance of Different Battery Pack Bottom Duct, *International Journal of Energy Research*, *42* (2018), 12, pp. 3823-3836
[9] Qu, J., *et al.*, Design and Experimental Study on a Hybrid Flexible Oscillating Heat Pipe, *International Journal of Heat and Mass Transfer*, *107* (2017), pp. 640-645
[10] Qu, J., *et al*., Heat Transfer Performance of Flexible Oscillating Heat Pipes for Electric/Hybrid-Electric Vehicle Battery Thermal Management, *Applied Thermal Engineering*, *135* (2018), 135
[11] Zhao, S., *et al.*, Development on Low-Temperature Performance of Lithium Ion Batteries, *Journal of the Chinese Ceramic Society*, *44* (2016), 1, pp. 19-28
[12] Gang, L. I., *et al*.. Design Research on Battery Heating and Preservation System Based on Liquid Cooling Mode, *Journal of Hunan University*, *44* (2017), 2, pp. 26-33
[13] Zhang, R., *et al*., Evaluation and Research on the High Performance 18650Btype Lithium Batteries of Rate and Low Temperature, *Chinese Battery Industry*, *20* (2016), 1, pp. 9-12
[14] Song, H. S., *et al*., Experimental Study on the Effects of pre-Heating a Battery in a Low-Temperature Environment, *Proceedings*, IEEE, Vehicle Power and Propulsion Conference, 2012, Seoul, Korea, pp. 1198-1201
[15] Shuai, X., *et al*., Study on Low Temperature Auxiliary Heat of Lithium Ion Battery, *Journal of Henan Science and Technology*, *22* (2015), 65
[16] Lei, Z., *et al*., Low-Temperature Performance and Heating Method of Lithium Battery in Electric Vehicles, *Journal of Beijing University of Technology*, *39* (2013), 9, pp. 1399-1404
[17] Luo, Y., *et al*., Study on Heating System of Lithium Ion Battery Pack in Low Temperature Environment *Journal of South China University of Technology (Natural Science Edition)*, *44* (2016), 9, pp. 100-106
[18] Stuart, T. A., Hande, A., The HEV Battery Heating Using AC Currents, *Journal of Power Sources*, *129* (2004), 2, pp. 368-378
[19] Salameh, Z. M., Alaoui, C., Modelling and Simulation of a Thermal Management System for Electric Vehicles, Industrial Electronics Society, *Proceedings*, 3th IECON '03. the, 3th Conference of the IEEE, IEEE, 2003, Vol. 1, pp. 887-890
[20] Li, B., *et al.*, Research on Influence of Preheating to Charging Character on Lithium Iron Phosphate Battery, *BUS and Coach Technology and Research*, *34* (2012), 3, pp. 25-27
[21] Pan, C., Guo, H., Study on EV Battery Pack Thermal Insulation And Heating, China Society of Automotive Engineers, *Proceedings*, Annual Conference of the Chinese Society of Automotive Engineers, Chinese Society of Automotive Engineers, Changsha, China, 2013, p. 4
[22] Zhang, C., *et al*., Method for Heating Low-Temperature Lithium Battery in Electric Vehicle, *Transactions of Beijing Institute of Technology*, *32* (2012), 9, pp. 921-925
[23] Bernardi, D., *et al.*, A General Energy Balance for Battery Systems, *Journal of the Electrochemical Society*, *132* (1984), 1, pp. 5-12
[24] Guo, Z., Mechanism and Control of Convective Heat Transfer – Coordination of Velocity and Heat Flow Fields, *Science Bulletin*, *46* (2001), 7, pp. 596-599
[25] Newman, J*., et al*., A General Energy-Balance for Battery Systems, *Journal of the Electrochemical Society*, *132* (1985), 1

Paper submitted: January 18, 2020
Paper revised: April 7, 2020
Paper accepted: April 13, 2020